https://doi.org/10.46813/2026-165-155

INTEGRATED METHODOLOGY FOR QUANTITATIVE ANALYSIS OF MICROSTRUCTURAL EVOLUTION IN POLYCRYSTALLINE MATERIALS WITH APPLICATION TO FUSION REACTOR MATERIALS

K.V. Pavlii*, O.F. Dyachenko, S.S. Herashchenko, V.A. Makhlai, O.V. Manuilenko, Yu.V. Petrov, B.V. Zajtsev
National Science Center "Kharkiv Institute of Physics and Technology", Kharkiv, Ukraine
****E-mail: kvint1@hotmail.com***

An integrated AI-driven digital morphometry methodology has been developed for the quantitative analysis of microstructural evolution in polycrystalline materials subjected to radiation–plasma exposure. The methodology combines automated SEM image segmentation using the MatSAM algorithm, statistical morphometric analysis, analytical modeling of grain morphology based on a two-parameter superellipse, and topological analysis of defect networks. The methodology was validated using polycrystalline tungsten in four characteristic conditions: the initial state, after helium-ion irradiation, after pulsed plasma exposure, and after their combined action. Quantitative indicators describing the transition from an initially isotropic microstructure to systematic surface fragmentation were identified. The proposed methodology provides an objective framework for the quantitative assessment of material degradation under the extreme operating conditions of fusion reactors.

PACS: 52.40.Hf; 52.70

INTRODUCTION

Polycrystalline tungsten is the primary candidate material for plasma-facing components (PFCs) in future fusion reactors owing to its exceptionally high melting point, low sputtering yield, high thermal conductivity, and excellent radiation resistance [1–3].

During reactor operation, tungsten is exposed to intense fluxes of energetic particles, giving rise to a complex sequence of degradation processes, including the formation of radiation-induced defects, the accumulation of internal stresses, nucleation of gas bubbles, formation of surface blisters**,** intergranular cracking, and progressive fragmentation of the near-surface microstructure [4–7]. The combined action of these processes ultimately determines the structural integrity, operational reliability, and service lifetime of plasma-facing components.

Scanning electron microscopy (SEM) remains the principal experimental technique for investigating radiation-induced changes in the microstructure of tungsten. However, despite its high spatial resolution, SEM image analysis is still predominantly qualitative. Microstructural evolution is commonly assessed by visual inspection, introducing operator-dependent bias and limiting the statistical reliability of the results. Furthermore, qualitative observations alone do not provide an objective basis for comparing successive stages of degradation or for establishing quantitative relationships between microstructural evolution and the underlying damage mechanisms [8–11].

1. CURRENT STATE OF THE ART

1.1. RADIATION-PLASMA DEGRADATION

Despite its outstanding thermophysical properties, tungsten undergoes progressive microstructural degradation under fusion-relevant operating conditions. The accumulation of radiation-induced defects leads to the formation of vacancies, self-interstitial atoms, and helium bubbles, accompanied by the development of residual stresses within the near-surface layer [4–6]. These processes progressively alter the surface morphology, promote intergranular cracking, and ultimately result in extensive surface fragmentation [7]. Quantitative assessment of these structural changes is therefore essential for reliable determination of material level degradation and prediction of service lifetime.

1.2. LIMITATIONS OF CONVENTIONAL CHARACTERIZATION METHODS

Scanning electron microscopy (SEM) remains the primary experimental technique for investigating radiation-induced surface degradation. However, quantitative interpretation of SEM micrographs has traditionally relied on manual image analysis, which suffers from several inherent limitations [12, 13]:

- limited statistical significance due to the relatively small number of analyzed grains;
- labor-intensive image processing;
- operator-dependent measurements and limited reproducibility.

As experimental datasets continue to increase in both size and complexity, these limitations have become a major obstacle to the development of reliable quantitative characterization methods for radiation-damaged materials.

1.3. EVOLUTION OF DIGITAL IMAGE ANALYSIS AND THE ROLE OF ARTIFICIAL INTELLIGENCE

Early automated image processing techniques, including threshold-based segmentation and conventional edge-detection algorithms, were effective only for relatively simple microstructures with high image contrast. Their application to irradiated tungsten is limited because SEM images typically contain numerous overlapping microstructural features, including grains,

helium bubbles, surface blisters, intergranular cracks, pores, and erosion regions.

A major advance has been achieved through the introduction of deep-learning foundation models for image segmentation. The Segment Anything Model (SAM) provides a versatile segmentation framework that can be adapted to a wide range of materials science applications [8]. Building upon this architecture, the MatSAM algorithm was developed for automated microstructural characterization, enabling the extraction of thousands of structural objects without retraining for each new SEM dataset. The introduction of foundation models has substantially improved segmentation accuracy, robustness, and statistical reliability compared with conventional image processing techniques [8–11]. The broader potential of foundation models for materials discovery has been reviewed in [14].

1.4. SCIENTIFIC GAP

Despite the rapid progress in AI-assisted microstructural characterization, most published studies remain focused on basic geometric descriptors, such as grain area and equivalent diameter, whereas grain orientation, crack-network topology, and the physical interpretation of quantitative morphometric parameters have received considerably less attention [15–17]. Furthermore, only a limited number of studies have proposed an integrated methodology capable of quantitatively describing the complete sequence of microstructural evolution: from the initial material state through helium-ion irradiation, hydrogen plasma exposure, and their combined action under fusion-relevant operating conditions [18]. Training-free segmentation of alloy microstructures via SAM has been demonstrated without additional model training [19].

To address this scientific gap, the present work proposes an integrated AI-driven methodology for quantitative analysis of microstructural evolution based on automated MatSAM segmentation, statistical morphometry, analytical grain-shape modeling, and topological characterization. The proposed methodology provides an objective and reproducible framework for the quantitative characterization of polycrystalline materials subjected to irradiation and thermal loading.

2. OBJECTIVES AND SCOPE OF THE STUDY

The primary objective of this study is to develop an AI-based methodology for quantitative analysis of the microstructural evolution of polycrystalline tungsten subjected to helium-ion irradiation, pulsed hydrogen plasma exposure, and their combined action under radiation and thermal loading conditions relevant to fusion reactors.

To achieve this objective, an automated analysis workflow based on SEM image segmentation using the MatSAM algorithm was developed. The proposed methodology provides statistically reliable analysis of large microstructural datasets while minimizing operator-dependent bias and ensuring high reproducibility of quantitative morphometric measurements [8–10].

The specific objectives of the study are:

- perform automated segmentation of SEM images representing four characteristic stages of degradation;
- quantitatively evaluate the evolution of grain geometry using morphometric descriptors, including grain area, perimeter, equivalent diameter, roundness, elongation ratio, and angularity coefficient;
- analyze grain orientation and its statistical evolution;
- perform quantitative analysis of intergranular crack-network topology;
- establish quantitative relationships among geometric, orientational, and topological descriptors at successive stages of degradation;
- identify quantitative indicators characterizing the transition from an initially isotropic microstructure to extensive surface fragmentation.

In contrast to conventional metallographic analysis, the proposed methodology integrates artificial intelligence, quantitative morphometry, statistical analysis, and topological analysis within a unified analytical framework. Although the methodology is demonstrated using polycrystalline tungsten, it is intended as a general approach for quantitative microstructural analysis of polycrystalline materials operating under irradiation and thermal loading.

3. MATERIALS AND EXPERIMENTAL PROCEDURE

3.1. MATERIAL

The investigated material was commercially available polycrystalline tungsten, widely used for plasma-facing components because of its high melting point, low sputtering yield, high thermal conductivity, and excellent radiation resistance [1–3]. The material was produced via powder metallurgy followed by thermomechanical processing, which accounts for the initial deformation texture observed in the reference state. The elemental composition of the investigated tungsten (W – 99.7%) includes the following impurities: Mo – 0.12%; Fe – 0.1%; with trace amounts of Na, Mg, S, and other elements. Prior to irradiation, the specimens were mechanically polished and chemically etched to remove the damaged surface layer and reveal a homogeneous reference microstructure for quantitative analysis. The average grain size of the initial material was approximately 23...25 μm, which is characteristic of recrystallized polycrystalline tungsten commonly employed in plasma-facing component research. Four characteristic microstructural states were investigated:

- S1 – initial state (polished and chemically etched);
- S2 – after helium-ion irradiation;
- S3 – after pulsed hydrogen plasma exposure;
- S4 – after helium ion irradiation followed by pulsed hydrogen plasma exposure.

This experimental design enables evaluation of both the individual and combined effects of irradiation and thermal loading on microstructural evolution.

3.2. HELIUM ION IRRADIATION

Helium-ion irradiation was performed using He^+ ions with an energy of 4 MeV at a fluence of $1.2 \cdot 10^{18}$ ions/cm^2 [4, 5, 17]. These conditions were

selected to reproduce near-surface radiation damage in plasma-inverted tungsten. Helium implantation promotes the formation of helium-vacancy complexes, bubble nucleation, and surface blistering, resulting in significant microstructural modification [4, 5, 7, 17]. These irradiated samples are designated as S2.

3.3. PULSED HYDROGEN PLASMA EXPOSURE

Hydrogen plasma exposure was performed using the QSPA Kh-50 quasi-stationary plasma accelerator. The irradiation mode consisted of 10 pulses with a pulse duration of 0.25 ms. The transient heat load was maintained at 0.9 MJ/m² per pulse, which simulates ELM-like (Edge Localized Mode) thermal shocks in fusion devices. The plasma stream was characterized by a diameter of approximately 6 cm, ensuring uniform exposure across the specimen surface. The resulting thermal stresses promoted initiation and propagation of intergranular cracks, leading to progressive fragmentation of the near-surface layer [6, 12, 13]. These samples are designated as S3.

3.4. COMBINED RADIATION-PLASMA TREATMENT

To investigate the synergistic effects of irradiation and thermal loading, a separate series of specimens was first irradiated with helium ions and subsequently exposed to pulsed hydrogen plasma under identical experimental conditions. This combined treatment produced the highest degree of structural degradation: radiation-induced defects acted as preferential crack-initiation sites, while thermally induced stresses accelerated crack propagation, resulting in extensive grain fragmentation and the formation of a highly interconnected crack network [6, 7, 13, 17]. These corresponding samples are designated as S4.

3.5. SCANNING ELECTRON MICROSCOPY

Surface morphology was examined using scanning electron microscopy (SEM) in secondary electron (SE) mode at an accelerating voltage of 15 kV. Micrographs were captured at a resolution of 1024×768 pixels with magnifications ranging from X100 to X3000. To ensure measurement consistency and direct quantitative comparison, identical imaging conditions and acquisition parameters were maintained for all specimens across the four investigated microstructural states (S1-S4).

4. AUTOMATED IMAGE SEGMENTATION AND DIGITAL MORPHOMETRY

4.1. AI-BASED IMAGE SEGMENTATION

Quantitative microstructural analysis was performed using an AI-based image analysis workflow built on the MatSAM segmentation algorithm, which employs the Segment Anything Model (SAM) as its foundation model and has been adapted for automated analysis of engineering materials [8–10]. MatSAM provides stable segmentation of complex SEM micrographs containing heterogeneous contrast, irregular grain morphology, radiation-induced defects, pores, and interconnected crack network, unlike conventional threshold-based or edge-detection techniques. All SEM images were processed automatically without manual grain-boundary delineation, enabling identification of grains, grain boundaries, pores, and crack-like objects as independent structural elements. The proposed workflow substantially increased both the number of analyzed objects and the statistical reliability of morphometric measurements compared with conventional manual metallographic procedures.

4.2. DIGITAL MORPHOMETRIC ANALYSIS

Following segmentation, each identified structural object was characterized using the following morphometric descriptors: grain area (A), perimeter (P), equivalent diameter (D), roundness (R), aspect ratio (AR), angularity coefficient, and orientation angle (θ). These descriptors characterize grain size, morphology, and preferred orientation. Grain area and perimeter describe the characteristic microstructural scale, whereas roundness and aspect ratio quantify deviations from an equiaxed morphology. The angularity coefficient reflects the development of faceted grain-boundary morphology, while the orientation angle provides a quantitative measure of texture evolution.

4.3. ANALYSIS OF GRAIN ORIENTATION

The preferred orientation of structural elements was determined from the major axis of each segmented grain. Orientation angles were measured relative to the horizontal direction and analyzed using probability density functions. Depending on the complexity of the microstructural state, the experimental distributions were approximated using either Gaussian or Gaussian mixture models. The transition from a unimodal to a bimodal orientation distribution was interpreted as evidence of increasing structural anisotropy during degradation.

To ensure strict spatial consistency and correct alignment of grain orientations, boundaries, and the crack network, reference marks (“anchors”) formed by molybdenum masks during the irradiation process were used as a unified reference system. This allowed for the correlation of statistical angle distributions with fixed specimen axes and the directions of external radiation-plasma exposure, ensuring identical measurement conditions for all series of micrographs.

4.4. CRACK NETWORK CHARACTERIZATION

In addition to grain morphology, intergranular crack network were quantitatively characterized using automated segmentation. Crack-like objects extracted from the SEM images were analyzed in terms of crack density, network connectivity, branching density, preferred crack orientation, and characteristic crack length. These descriptors characterize the structural integrity of the near-surface layer and quantitatively describe the transition from isolated defects to an interconnected crack network. Their evolution was analyzed together with grain morphology to establish relationships between crack propagation and grain fragmentation.

The use of the “anchor” reference marks and molybdenum masks ensured strict spatial alignment during the analysis of crack-network anisotropy across all experimental series. This data coupling guaranteed that the preferred crack orientation was measured in the same coordinate system as the grain orientations,

allowing for a direct correlation between fracture propagation directions and the vectors of external radiation-plasma exposure. However, it should be emphasized that this technical alignment does not affect the mathematical framework or the underlying algorithms of the subsequent calculations.

4.5. STATISTICAL ANALYSIS

To ensure statistical reliability, thousands of structural objects were analyzed for each experimental condition. Morphometric parameters were described using probability density functions. Depending on the parameter under consideration, Gaussian, log-normal, or Gaussian mixture models were employed. Mean values, standard deviations, distribution widths, and confidence intervals were calculated for all descriptors. Distribution fitting was performed using the maximum likelihood method, while the goodness of fit was evaluated using standard statistical criteria. This statistical framework enabled objective comparison of the four microstructural states (S1-S4) while minimizing uncertainties associated with manual image interpretation.

4.6. INTEGRATED MORPHOMETRIC FRAMEWORK

The principal advantage of the proposed methodology lies in the integration of automated image segmentation, quantitative morphometry, grain orientation analysis, and crack network topology analysis within a unified analytical framework. Unlike conventional metallographic approaches based on a limited set of geometric parameters, the proposed methodology simultaneously evaluates complementary groups of descriptors that quantitatively characterize microstructural evolution, enabling the transition from qualitative interpretation of SEM micrographs to statistically reliable quantitative analysis of degradation processes and providing a robust framework for correlating radiation damage, thermal loading, and microstructural evolution [9–11, 20].

The integration of the AI-based methodology lies in its ability to simultaneously process multiple data levels. Unlike conventional methods, the proposed workflow uses a single AI-driven segmentation source to construct a multidimensional degradation profile, where geometric, orientation, and topological descriptors are not analyzed in isolation but as interrelated variables of a single physical process of surface destruction.

5. RESULTS AND DISCUSSION

5.1. EVOLUTION OF SURFACE MORPHOLOGY

Automated SEM image segmentation enabled the progressive evolution of the tungsten surface morphology to be traced throughout the four investigated microstructural states (S1-S4). Representative segmented microstructures are presented in Figure. The angle indicated in Figure represents the dominant orientation angle (μ_θ) of the structural elements. It was measured as the inclination of the major axis of each segmented object relative to the horizontal axis of the image. To ensure strict spatial consistency across the S1-S4 series, the horizontal direction was strictly referenced to the specimen axes using reference marks (“anchors”) formed by molybdenum masks during the irradiation process. The initial material (S1) exhibits a homogeneous polycrystalline microstructure consisting of nearly equiaxed grains with smooth grain boundaries.

Following helium-ion irradiation (S2), the microstructure undergoes noticeable morphological modifications. The formation of surface blisters becomes evident, while grain boundaries become increasingly irregular owing to localized radiation-induced deformation. Although the overall grain topology remains largely unchanged, the appearance of isolated damaged regions indicates the onset of structural degradation [4, 5, 7, 17].

Exposure to pulsed hydrogen plasma (S3) produces more pronounced structural changes. Numerous intergranular microcracks develop across the surface, accompanied by progressive faceting of grain boundaries and increasing morphological anisotropy. Compared with the helium-irradiated condition, crack density increases markedly, indicating that thermal loading becomes the dominant degradation mechanism under these conditions [6, 12, 13].

The combined action of helium-ion irradiation and pulsed hydrogen plasma (S4) results in the highest degree of structural degradation. The crack network becomes highly interconnected, the grain structure undergoes extensive fragmentation into smaller structural units, and the original microstructure is partially destroyed. Surface fragmentation is accompanied by increased structural heterogeneity, reflecting the synergistic interaction between radiation-induced defects and plasma-induced thermal stresses [6, 7, 13, 17].

These observations demonstrate that tungsten degradation proceeds through a sequence of distinct microstructural stages rather than as a continuous random process. Each stage is characterized by specific morphological features that can be quantitatively described using the proposed AI-based methodology.

5.2. QUANTITATIVE ANALYSIS OF GRAIN GEOMETRY

The quantitative morphometric parameters of the grain structure are summarized in Table 1. The values are presented as Mean ± Standard Error of the mean (SEM). The analysis revealed a non-monotonic evolution of the average grain area during progressive degradation.

Table 1

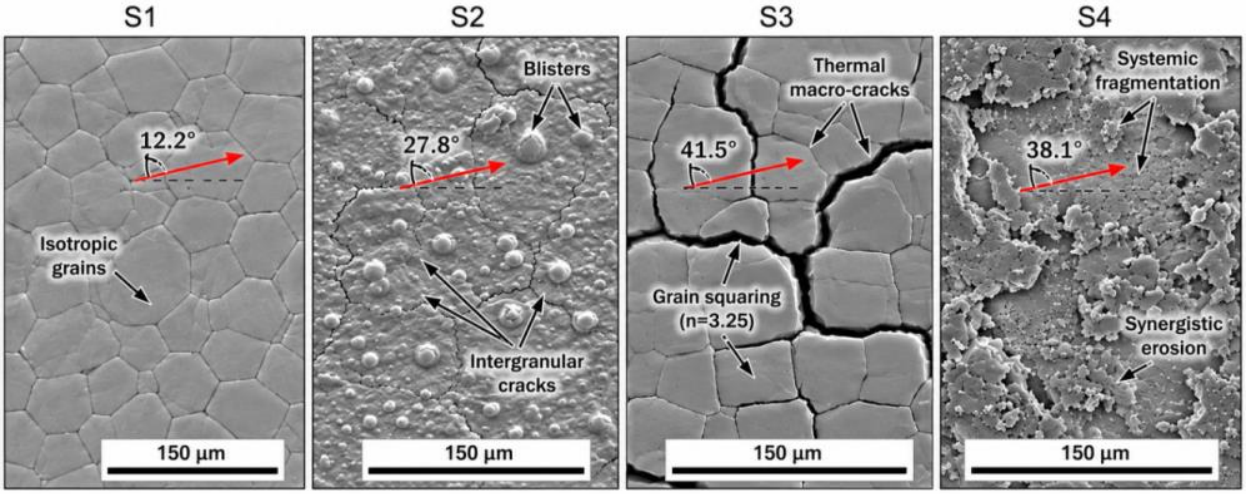
Morphometric parameters of the grain structure. The values are presented as Mean ± Standard Error of the mean (SEM)

Series	Area A, μm²	Perimeter P, μm
S1	452.1±12.4	78.4±5.1
S2	520.4±18.2	89.6±6.3
S3	480.2±22.5	114.3±8.7
S4	415.7±14.8	106.8±7.2

In the reference state (S1), the average grain area was 452.1 μm², while the corresponding average perimeter was 78.4 μm. Following helium ion irradiation (S2), the average grain area increased to 520.4 μm², indicating radiation-induced swelling of the near-surface layer. Simultaneously, the average grain perimeter increased to

89.6 μm, reflecting the increasing complexity of grain-boundary morphology.

For the S3 series, the average grain area decreased to 480.2 μm², whereas the average perimeter increased to 114.3 μm, indicating enhanced boundary tortuosity associated with the development of an intergranular crack network.



Evolution of surface morphology and damage anisotropy under radiation and thermal loading

Following combined radiation-plasma exposure (S4), the average grain area decreased further to 415.7 μm², while the average perimeter remained relatively high (106.8 μm). This combination of changes indicates the transition to the fragmentation stage, during which previously deformed grains are subdivided into smaller structural fragments. The grain area and perimeter distributions for all experimental series were described using the lognormal probability density function:

$$f(x;\mu,\sigma) = \frac{1}{x\sigma\sqrt{2\pi}}\exp\left(-\frac{(\ln x-\mu)^2}{2\sigma^2}\right), \qquad (1)$$

where x denotes the measured morphometric parameter (grain area A or perimeter P), μ is the scale parameter (the mean of the logarithmic variable), and σ is the shape parameter (the corresponding standard deviation). The fitted parameters are summarized in Table 2.

Table 2

Parameters of the lognormal distribution for grain area (A) and perimeter (P)

Series	Area		Perimeter	
	μ_A	σ_A	μ_P	σ_P
S1	6.11	0.15	4.36	0.12
S2	6.25	0.28	4.50	0.21
S3	6.17	0.35	4.74	0.30
S4	6.03	0.18	4.67	0.14

For the S1 series, the shape parameter σ_A was 0.15, corresponding to a relatively narrow grain-size distribution. Following helium ion irradiation, σ_A increased to 0.28, indicating increased microstructural heterogeneity associated with radiation-induced swelling [5, 6]. The broadest distribution was observed for the S3 series (σ_A = 0.35), corresponding to the highest degree of morphological heterogeneity [12, 13]. For the S4 series, σ_A decreased to 0.18; however, this reduction reflects the fragmentation of previously deformed grains into more uniform structural fragments rather than recovery of the original microstructure [18, 20].

These results indicate that the maximum level of microstructural heterogeneity is reached after pulsed hydrogen plasma exposure (S3), immediately preceding the onset of extensive surface fragmentation [5, 16].

5.3. EVOLUTION OF GRAIN SHAPE PARAMETERS

To analytically describe grain contours, a rotated asymmetric two-parameter superellipse model was employed:

$$(x'/a)^n + (y'/b)^k = 1, \qquad (2)$$

where $x' = x\cos\theta + y\sin\theta$, $y' = -x\sin\theta + y\cos\theta$; a and b are the major and minor semi-axes defining the grain size and aspect ratio, respectively; θ is the orientation angle specifying the preferred direction of grain deformation; n and k are the superellipse exponents describing the curvature of grain boundaries; and $|n-k|$ serves as an indicator of degradation nonuniformity and local stress concentration along grain boundaries.

The corresponding shape parameters are summarized in Table 3, demonstrating a pronounced dependence on the degradation stage.

Table 3

Grain shape parameters

Series	n	k	|n-k|	AR
S1	2.02	2.01	0.01	1.11
S2	1.94	1.90	0.04	1.15
S3	1.86	1.70	0.16	1.41
S4	1.72	1.62	0.10	1.33

In the initial state, the shape parameters n and k are close to 2, corresponding to nearly elliptical grain contours. Following helium-ion irradiation, both parameters decrease, whereas the difference $|n-k|$ remains relatively small. The most pronounced changes are observed for the S3 series, where $|n-k|$ reaches 0.16, indicating pronounced morphological anisotropy and the formation of localized regions with increased grain-boundary curvature. For the S4 series, $|n-k|$ decreases to 0.10; however, the absolute values of both n and k remain

substantially lower than those of the initial material, indicating that the complex grain-boundary geometry persists even after structural fragmentation. The increased aspect ratio (1.41) in the S3 series further confirms the formation of elongated anisotropic structural fragments characteristic of maximum morphological instability.

5.4. GRAIN ORIENTATION DISTRIBUTION

The statistical distribution of grain orientation angles for each experimental series was described using a Gaussian probability density function:

$$f(\theta) = \frac{1}{\sigma_\theta \sqrt{2\pi}} \exp\left(-\frac{(\theta - \mu_\theta)^2}{2\sigma_\theta^2} \right), \qquad (3)$$

where μ_θ is the dominant orientation angle (the position of the distribution maximum), representing the preferred grain alignment direction, and σ_θ is the standard deviation (distribution width), characterizing the spread of grain orientations and, consequently, the degree of texture dispersion. The fitted parameters are summarized in Table 4.

Table 4

Parameters of the orientation distribution

Series	μ_θ, degree	σ_θ, degree	f_{max}
S1	12.2	8.2	0.0487
S2	27.8	12.5	0.0319
S3	41.5	15.1	0.0264
S4	38.1…40.1	10.4	0.0384

The dominant orientation angle progressively shifts from 12.2° in the initial state to 41.5° after pulsed hydrogen plasma exposure, indicating continuous microstructural reorientation. At the same time, the standard deviation increases from 8.2 to 15.1°, reflecting the increasing spread of grain orientations and progressive degradation of the original texture. Following combined radiation-plasma exposure, the distribution width decreases to 10.4°, whereas the dominant orientation remains within the range of 38…40°. This behavior indicates stabilization of the fragmented microstructure accompanied by the preferential alignment of structural fragments along the dominant crack propagation directions. The minimum value of the maximum probability density (f_{max} = 0.0264) was observed for the S3 series, corresponding to the highest degree of texture degradation.

5.5. TOPOLOGY OF GRAIN BOUNDARIES AND CRACK NETWORK

Topological analysis revealed a progressive increase in the complexity of grain-boundary and crack-network structures as microstructural degradation advanced. For the S2 series, the number of localized defects and isolated cracks increased. In the S3 series, both the density of crack branching nodes and the total crack-network length increased significantly. The most complex topology was observed for the S4 series, where individual cracks merged into a highly interconnected network. The increasing network connectivity was accompanied by the formation of preferential fracture paths and the subdivision of previously deformed grains into smaller structural fragments.

These results indicate that the topological characteristics of grain boundaries and crack network represent the most sensitive indicators of the transition from localized damage accumulation to extensive surface fragmentation.

6. DISCUSSION

The present study demonstrates that the proposed AI-based methodology provides a unified analytical framework for the quantitative analysis of microstructural evolution in polycrystalline materials operating under fusion-relevant irradiation and thermal loading conditions. Unlike conventional SEM image analysis, which is typically limited to qualitative observations or a small number of geometric descriptors, the proposed methodology integrates automated image segmentation, statistical morphometry, analytical grain-shape modeling, and topological analysis into a single quantitative workflow. This integration enables a transition from the isolated evaluation of individual morphological features to a comprehensive quantitative description of microstructural degradation processes.

Application of the proposed methodology to polycrystalline tungsten enabled the identification of successive stages of radiation- and plasma-induced degradation. Independent analyses of grain geometry, grain orientation distributions, and crack-network topology consistently revealed the transition from localized damage accumulation to extensive surface fragmentation. The strong agreement among these complementary descriptor groups confirms the reliability and reproducibility of the proposed methodology for quantitative microstructural characterization. Importantly, each descriptor group captures different aspects of structural degradation, while their combined analysis substantially improves the reliability of interpreting the underlying degradation mechanisms.

The proposed methodology provides an integral assessment by identifying the correlation between different descriptor groups. A key indicator of the material's state is the coupling between the increase in grain anisotropy (the |n-k| parameter) and the crack network branching density. This synergy allows for the quantitative identification of the bifurcation point – the moment when localized damage accumulation (Series S2) transitions into systemic surface fragmentation (Series S4).

A key advantage of the proposed approach lies in the simultaneous use of several complementary groups of descriptors. Whereas conventional morphometric parameters provide only partial information about structural evolution, their integration with orientation and topological descriptors enables a considerably more comprehensive interpretation of degradation mechanisms under combined irradiation and thermal loading. Consequently, the proposed methodology quantitatively characterizes not only changes in grain size and morphology but also the spatial organization of the microstructure, the evolution of structural anisotropy, and the formation of interconnected crack networks as interrelated stages of a single degradation process.

The rotated asymmetric two-parameter superellipse provided an efficient analytical representation of grain

morphology, whereas statistical analysis of grain orientations enabled quantitative evaluation of structural anisotropy evolution. At the same time, topological descriptors of grain boundaries and crack networks proved to be the most sensitive indicators of the transition from localized damage accumulation to extensive surface fragmentation. Together, these complementary analyses establish objective quantitative criteria for distinguishing successive stages of material degradation. Unlike most existing approaches, which focus primarily on individual morphometric parameters, the proposed methodology considers the microstructure as an integrated system whose evolution is governed by the coupled variation of geometric, orientation, and topological characteristics.

Although the methodology has been demonstrated using polycrystalline tungsten as a representative plasma-facing material, it is not material-specific. Because it is based on automated SEM image analysis, the proposed approach can readily be adapted for the quantitative characterization of a wide range of polycrystalline metals, alloys, ceramics, composites, and protective coatings subjected to irradiation, thermal, mechanical, plasma, or combined extreme loading conditions. This broad applicability significantly extends its potential beyond fusion materials research [21]. The methodology can therefore serve as a general platform for quantitative investigations of microstructural evolution in a broad class of polycrystalline materials, irrespective of the external loading nature.

In summary, the proposed methodology represents not only an effective tool for automated microstructural characterization but also a foundation for intelligent structural diagnostics, quantitative degradation assessment, and predictive evaluation of the structural integrity and service life of engineering materials operating under extreme conditions. Furthermore, the developed approach provides a basis for future AI-assisted systems for structural health monitoring based on the integrated analysis of morphological, orientation, and topological microstructural features, thereby contributing to improved reliability and lifetime prediction of advanced engineering materials operating in extreme environments.

CONCLUSIONS

• An integrated artificial-intelligence-based methodology for the quantitative analysis of the microstructure of polycrystalline materials has been developed. The methodology combines automated SEM image segmentation, statistical morphometry, analytical grain-shape modeling using a rotated asymmetric two-parameter superellipse model, and topological analysis of grain-boundary and crack networks within a unified analytical framework.

• The methodology was successfully validated using polycrystalline tungsten subjected to helium-ion irradiation, pulsed hydrogen plasma exposure, and their combined action under radiation and thermal loading. The proposed analytical workflow provides an objective quantitative characterization of successive degradation stages through changes in grain geometry, grain orientation, and crack-network topology.

• It has been demonstrated that the rotated asymmetric two-parameter superellipse model provides an efficient analytical representation of grain morphology. The resulting model parameters enable the quantitative characterization of grain-shape evolution and the development of structural anisotropy during material degradation.

• The combined use of morphometric, statistical, and topological descriptors has been shown to provide substantially higher sensitivity to microstructural evolution than conventional geometric parameters considered individually. Among the investigated characteristics, crack-network topology proved to be the most sensitive indicator of the transition from localized damage accumulation to extensive surface fragmentation.

• The scientific novelty of this work lies in the development of a unified analytical framework that transitions from isolated geometric measurements to a multidimensional quantitative description of microstructural evolution. Unlike existing approaches, the proposed methodology integrates AI-driven segmentation, analytical grain-shape modeling using a two-parameter superellipse, and topological characterization of crack networks into a single diagnostic cycle. A key novel result is the identification of a quantitative “degradation trajectory”, where the coupling between grain-boundary tortuosity, the asymmetry of the superellipse (|n-k| parameter), and the branching density of the crack network serves as an objective indicator of the transition from localized damage to systemic surface fragmentation. The use of reference "anchors" further ensures that these complex structural changes are strictly correlated with the vectors of external radiation-plasma exposure, providing a level of spatial consistency not previously achieved in automated SEM analysis.

• The proposed methodology has broad applicability. In addition to polycrystalline tungsten, it can be applied to the quantitative microstructural characterization of metals, alloys, ceramics, composites, protective coatings, and other engineering materials operating under radiation, thermal, mechanical, plasma, or combined extreme loading conditions. The methodology provides a scalable foundation for automated microstructural characterization, structural integrity assessment, and service-life prediction of engineering materials operating in extreme environments.

REFERENCES

1. G. Federici, C.H. Skinner, J.N. Brooks, et al. Key issues for plasma-facing components in ITER // *Journal of Nuclear Materials*. 2003, v. 313-316, p. 11-22.

2. G. Pintsuk. Tungsten as a plasma-facing material // *Journal of Nuclear Materials.* 2013, v. 438, S2-S10.

3. Y. Ueda, N. Yoshida, S. Kajita, et al. Recent progress of tungsten research for plasma-facing components in fusion devices // *Nuclear Fusion*. 2014, v. 54, p. 013006.

4. J.A.R. Wright. A review of late-stage tungsten fuzz growth // *Tungsten*. 2022, v. 4, p. 184-193.

5. S. Kajita, T. Saeki, Y. Hirahata, N. Ohno. Formation of metallic nanostructure by helium plasma irradiation // *Japanese Journal of Applied Physics*. 2011, v. 50, 01AH02.

6. H. Takata, N. Yoshida, S. Yamanaka, et al. An inter-bubble fracture mechanism of blister formation on helium-irradiated metals // *Acta Materialia*. 2003, v. 51, p. 3071-3077.

7. N. Yoshida, S. Kajita, N. Ohno, et al. Helium effects on tungsten surface morphology and deuterium retention // *Journal of Nuclear Materials*. 2014, v. 454, p. 390-395.

8. A. Kirillov, E. Mintun, N. Ravi, et al. Segment Anything // *Proc. IEEE/CVF Int. Conf. Comput. Vis. (ICCV).* 2023, p. 3992-4003.

9. C. Li, X. Han, C. Yao, Y. Guo, et al. A novel training-free approach to efficiently extracting material microstructures via visual large model // *Acta Materialia*. 2025, v. 290, 120962.

10. K. Barmak, J.M. Rickman, S. Takeuchi, et al. Machine learning for materials microstructures: A survey of applications and methodologies // *Acta Materialia*. 2026, v. 308, 122041.

11. M. Wittwer, B. Eryilmaz, M. Santangelo, et al. An automated and unbiased grain segmentation method based on directional reflectance microscopy // *Materials Characterization*. 2021, v. 174, 110978.

12. A. Bakaeva, I. Garkusha, V. Makhlai, et al. Correlation of hardness and surface microcracking in ITER specification tungsten exposed at QSPA Kh-50 // *Journal of Nuclear Materials*. 2019, v. 520, p. 185-192.

13. I.E. Garkusha, V.A. Makhlai, B.N. Bazylev, et al. Tungsten melt losses under QSPA Kh-50 plasma exposures simulating ITER ELMs and disruptions // *Fusion Science and Technology*. 2014, v. 65, p. 186-193.

14. E.O. Pyzer-Knapp, M. Manica, P. Staar, et al. Foundation models for materials discovery – current state and future directions // *npj Computational Materials*. 2025, v. 11, Art. 61.

15. M. Richou, A. Durif, S. Miro, et al. A comparative study on the in situ helium irradiation behavior of tungsten: coarse grain vs. nanocrystalline grain // *Acta Materialia.* 2018, v. 147, p. 100-112.

16. N. Gao, M.H. Cui, W. Setyawan, R.J. Kurtz. Loop-punching suppression induced by growth of helium bubble pair in tungsten // *Journal of Applied Physics*. 2018, v. 124, 235105.

17. T. Wang, Y. Zhang, H. Li, et al. Helium retention, bubble superlattice formation and surface blistering in helium-irradiated tungsten // *Journal of Nuclear Materials.* 2021, v. 545, 152722.

18. M.J. Patrick, K. Barmak. Automated grain boundary detection for bright-field transmission electron microscopy images via U-Net // *Microscopic Microanalysis.* 2023, v. 29, p. 1968-1981.

19. X. Ma, Y. Zhang, C. Wang, W. Xu. Alloy microstructure segmentation through SAM and domain knowledge without extra training // *Scripta Materialia*. 2025, v. 260, 116581.

20. V.I. Butenko, O.F. Dyachenko, I.E. Garkusha, et al. Correlations between morphometric parameters and surface defects of tungsten under radiation-thermal exposure // *Problems of Atomic Science and Technology*. 2026, № 3(163), p. 180-187.

21. R. Bostanabad, W. Chen, J. Chan, et al. Computational microstructure characterization and reconstruction: Review of the state-of-the-art techniques // *Progress in Materials Science*. 2018, v. 95, p. 1-41.

Article received 02.10.2026

ІНТЕГРОВАНА МЕТОДОЛОГІЯ ДЛЯ КІЛЬКІСНОГО АНАЛІЗУ ЕВОЛЮЦІЇ МІКРОСТРУКТУРИ ПОЛІКРИСТАЛІЧНИХ МАТЕРІАЛІВ ІЗ ЗАСТОСУВАННЯМ ДО МАТЕРІАЛІВ ТЕРМОЯДЕРНИХ РЕАКТОРІВ

К.В. Павлій, О.Ф. Дьяченко, С.С. Геращенко, В.О. Махлай, О.В. Мануйленко, Ю.В. Петров, Б.В. Зайцев

Розроблено інтегровану методологію цифрової морфометрії на основі штучного інтелекту для кількісного аналізу еволюції мікроструктури полікристалічних матеріалів, що зазнають радіаційно-плазмового впливу. Методологія поєднує автоматизовану сегментацію СЕМ-зображень із використанням алгоритму MatSAM, статистичний морфометричний аналіз, аналітичне моделювання форми зерен на основі двопараметричної супереліпси та топологічний аналіз мереж дефектів. Методологію апробовано на полікристалічному вольфрамі в чотирьох характерних станах: первинному, після опромінення іонами гелію, після впливу імпульсної плазми та після їх комбінованої дії. Визначено кількісні індикатори переходу від початково ізотропної мікроструктури до системної фрагментації поверхні. Запропонована методологія забезпечує об’єктивну основу для кількісної оцінки деградації матеріалів у екстремальних умовах експлуатації термоядерних реакторів.